Structure and electronic properties of Ge_n $(n=2-25)$ clusters from density-functional theory

Jinlan Wang,[1,2] Guanghou Wang,[1,*] and Jijun Zhao[3,†]
[1]*National Laboratory of Solid State Microstructures and Department of Physics, Nanjing University, Nanjing 210093, China*
[2]*Department of Physics, Guangxi University, Nanning 530004, China*
[3]*Department of Physics and Astronomy, University of North Carolina at Chapel Hill, Chapel Hill, North Carolina, 27599-3255*
(Received 9 May 2001; published 31 October 2001)

The geometrical and electronic structures of the germanium clusters with up to 25 atoms are studied by using density-functional theory with the generalized gradient approximation. The Ge_n clusters follow a prolate growth pattern with $n \geqslant 13$. For medium-sized clusters, we find two kinds of competing structures, stacked layered structures and compact structures. The stacked layered structures with capped tetrahedron Ge_9 cluster are more stable than compact structures and other stacked structures. The size dependence of cluster binding energies, highest-occupied and lowest-unoccupied molecular orbital gap, and ionization potentials are discussed and compared with experiments.

DOI: 10.1103/PhysRevB.64.205411 PACS number(s): 36.40.Cg, 36.40.Mr, 61.46.+w

I. INTRODUCTION

Clusters containing a few to thousands of atoms consist of an intermediate regime between individual atoms and bulk solids.[1,2] In this regime, the physical and chemical properties of clusters are size dependent. Thus, clusters are often considered as a bridge for a comprehensive understanding as to how matter evolves from atoms to bulk. During the past two decades, the group-IV semiconductor clusters have been intensively studied both experimentally[3–13] and theoretically[14–27] because of their fundamental importance and potential applications in nanoelectronics. So far, the structures and properties of small silicon and germanium clusters $(n=2-7)$ are already well understood. But our knowledge of the Ge_n clusters with $n>10$ are still quite limited. For example, previous experimental and theoretical studies have suggested that small germanium clusters may adopt highly coordinated compact structures that are totally different from the bulk diamond structure. The rearrangement from small compact structures into a bulklike diamond lattice in germanium clusters is still an open question.

Experimental works on germanium clusters include atomization energies,[3] mass spectra,[4–6] photofragmentation,[7] photoionization,[8] photoelectron spectroscopy[9,10] and electronic gap,[11] ion mobility measurement,[13] etc. In particular, ion mobility measurements suggest that the germanium clusters adopt the prolate growth pattern up to $n\sim 70$. Previous theoretical works based on tight-binding molecular dynamics[18–20] (TBMD) or *ab initio* methods[21–27] are focused on the lowest-energy structures and electronic structures. Among those studies, accurate first-principles calculations are usually limited in small cluster size $(n\leqslant 13)$.

In this paper, we explore the lowest-energy structures of germanium clusters and investigate their electronic properties including highest-occupied and lowest-unoccupied molecular orbital (HOMO-LUMO) gap and ionization potentials (IP's) using density-functional theory (DFT) with a generalized gradient approximation (GGA). The equilibrium structures of Ge_n clusters are determined from a number of structural isomers, which are generated from genetic algorithm simulations based on a nonorthogonal tight-binding (NTB) model.[19]

II. METHODS

Density-functional electronic structure calculations on Ge_n $(n=2-25)$ clusters have been performed by using the DMOL package.[28] During the density-functional calculations, the effective core potential and a double numerical basis including the *d*-polarization function are chosen. The density functional is treated by generalized gradient approximation[29] with exchange-correlation potential parametrized by Wang and Perdew.[30] Self-consistent field calculations are carried out with a convergence criterion of 10^{-6} a.u. on the total energy and electron density. Geometry optimizations are performed with the Broyden-Fletcher-Goldfarb-Shanno (BFGS) algorithm. We use a convergence criterion of 10^{-3} a.u. on the gradient and displacement and 10^{-5} a.u. on the total energy in the geometry optimization.

The determination of ground-state structures is one of the most fundamental and challenging problems in cluster physics due to the numerous isomers in configuration space. The most commonly used strategy in searching the lowest-energy structures of small clusters with reliable accuracy is the simulated annealing (SA) scheme based on density-functional calculations. However, the well-known NP leads to a computation that is expensive for clusters with $n\geqslant 10$. Alternatively, we perform an unbiased global search of the cluster low-energy isomers by using genetic algorithm[31–33] based on NTB molecular dynamics.[19] Our essential idea is to divide the phase space into a number of regions and find a locally stable isomer to represent each of them. It is already proven that the NTB scheme can give a good description of germanium clusters.[19] Thus, these minima are expected to make a reasonable sampling of the phase space and can be further optimized by DFT. If there is no significant difference between the DFT and tight-binding phase space, the global minimal configuration at the GGA level should be achieved by such a combination of NTB-GA search and GGA minimization.

TABLE I. Lowest-energy configurations and electronic properties of Ge_n clusters. E_b^a (eV): theoretical binding energy per atom. E_b^b: experimental binding energy per atom (Refs. 3 and 13) [for Ge_{2-8}, measured atomization energy (Ref. 3); for Ge_{9-19}, estimation from ion mobility (Ref. 13)]. IP^a (eV): theoretical vertical IP's. IP^b (eV): experimental IP's (Ref. 8). Δ (eV): theoretical HOMO-LUMO gap.

n	Geometry	E_b^a	E_b^b	IP^a	IP^b	Δ
2	Dimer	1.23	1.35	7.53	7.67	2.07
3	Isosceles triangle	2.24	2.04	7.83	8.03	1.32
4	Rhombus	2.70	2.53	7.52	7.92	1.11
5	Trigonal bipyramid	2.91	2.72	7.77	7.92	2.23
6	Distorted octahedron	3.05	2.85	7.64	7.67	2.32
7	Pentagonal bipyramid	3.22	2.97	7.60	7.67	1.81
8	Capped pentagonal bipyramid	3.16	3.06	6.78	6.83	1.09
9	Bicapped pentagonal bipyramid	3.24	3.04	6.83	7.15	1.63
10	Tetracapped trigonal prism	3.33	3.13	7.13	7.61	1.82
11	Bicapped square antiprism	3.27	3.13	6.45	6.64	0.91
12	Distorted icosahedron	3.26	3.21	6.63	7.00	1.70
13	Layered structure	3.29	3.12	6.58	7.00	1.16
14	Layered structure	3.34	3.14	6.63	7.15	1.52
15	Layered structure	3.34	3.15	6.46	7.15	0.88
16	Layered structure	3.35	3.17	6.58	6.83	1.37
17	Layered structure	3.31	3.15	6.24		0.83
18	Stacked layered structure	3.34	3.15	6.33	6.63	1.12
19	Near-spherical compact structure	3.31	3.15	6.12	6.40	0.66
20	Stacked layered structure	3.33		6.32	6.40	1.16
21	Stacked layered structure	3.34		6.13	6.32	0.99
22	Compact structure	3.32		6.00	6.00	0.68
23	Compact and stacked structure	3.34		6.08	6.00	0.90
24	Compact and stacked structure	3.34		5.91	5.94	0.57
25	Compact and stacked structure	3.34		5.83	5.94	0.63

III. LOWEST-ENERGY STRUCTURES OF GERMANIUM CLUSTERS

The obtained lowest-energy structures of germanium clusters are described in Table I and Fig. 1. The binding energy of the Ge_2 dimer is 1.23 eV, which agrees well with the experimental value (1.32 eV)[3]. The Ge_3 is an isosceles triangle (C_{2v}) with bond length 2.40 Å and apex angle $\theta = 84.9°$. For the Ge_4, the lowest-energy structure is a D_{2h} rhombus with side length 2.55 Å and minor diagonal length 2.76 Å. Trigonal bipyramid (D_{3h}) and distorted octahedron (D_{2h}) are obtained for Ge_5 and Ge_6. The most stable geometries for Ge_7, Ge_8, and Ge_9 are pentagonal bipyramid (D_{5h}), capped pentagonal bipyramid and bicapped pentagonal bipyramid, respectively. The configuration of Ge_8 and Ge_9 can be easily understood as growth on the basis of Ge_7. Thus, it is not surprising that the Ge_7 is more stable than the Ge_8 and Ge_9 clusters. In the case of the Ge_{10}, our calculations suggest that the tetracapped trigonal prism (C_{3v}) has favorable energy. The current structures for small Ge_n ($n = 3-10$) clusters are consistent with previous DFT calculations.[17,25,27] Moreover, as shown in Table I, our theoretical cohesive energies of the Ge_n clusters agree very well with the experimental data. Therefore, we believe that the present DFT-GGA scheme has made a successful prediction of the germanium clusters and can be further applied to the larger systems.

For Ge_n with $n > 10$, there are few first-principles calculations on the equilibrium structures of the clusters. Shvartsburg *et al.* compared germanium and silicon clusters up to 16 with local density approximation (LDA) calculations.[17] But the initial geometries of the germanium clusters with $n > 13$ come from those of silicon clusters, which might not give an accurate description of the configuration space of the medium-sized germanium clusters. From our calculations, the lowest-energy structure for Ge_{11} is a bicapped square antiprism with an additional face-capped atom, which was

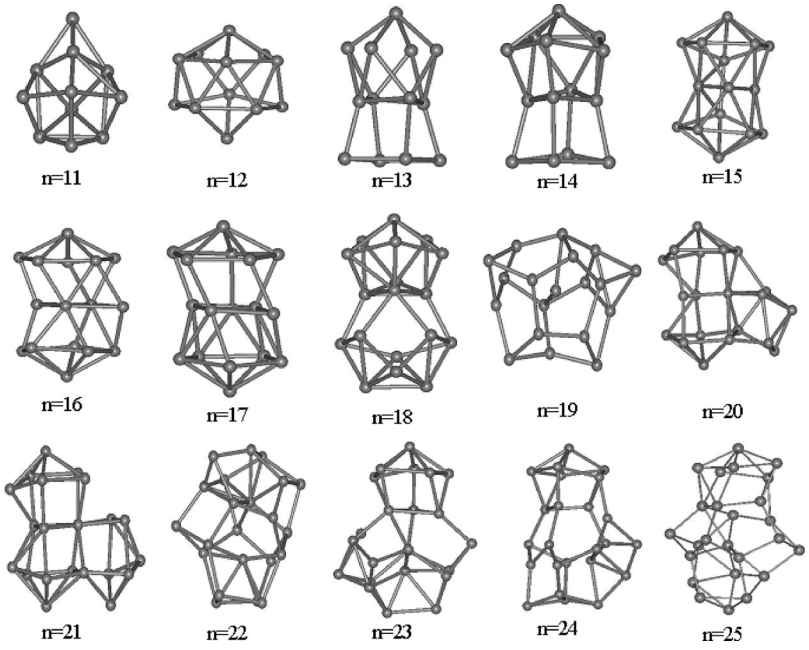

FIG. 1. Lowest-energy structures for Ge_n ($n = 11-25$) clusters.

previously obtained by Lu *et al.*[27] For Ge_{12}, the most stable structure is a strongly distorted icosahedron (I_h), which is different from the C_{2v} geometry found by Shvartsburg *et al.*[17] For the Ge_n clusters with $n \geqslant 13$, the lowest-energy structures follow a prolate pattern with stacks of small unit clusters, which are forming layered structures. For example, the lowest-energy structure for Ge_{13} consists of a square Ge_4 subunit and a capped tetragonal prism Ge_9. This structure can be understood as 1-5-3-4 layers. A similar 1-5-4-4 layered structure is obtained for Ge_{14}. In comparison with Ge_{13}, the Ge_9 unit is replaced by a bicapped square antiprism Ge_{10} in the case of Ge_{14}. Our present results suggest a structural transition from spherical configuration to prolate layered structures around $n=13$.

The lowest-energy structure of Ge_{15} is a stacked structure with 1-5-3-5-1 layers. Similar stacked structures are obtained for Ge_{16} and Ge_{17} as 1-5-4-5-1 or 1-5-5-5-1 layers. The layered structures have also been found in medium-sized silicon and germanium clusters by Shvartsburg *et al.*[17] These equilibrium structures for Ge_n and Si_n ($n=13$–17) imply that formation of layers with four- or five-member rings is the dominant growth pattern of these medium-sized clusters. However, such a structural pattern does not continue at Ge_{18} and Ge_{19}. Alternatively, Ge_{18} consists of two interpenetrated pentagons connected with a bicapped square antiprism Ge_{10} subunit. A cagelike configuration with higher compactness is obtained for Ge_{19}, which is also similar to that obtained for Si_{19}.[34] The prolate stacked layer structures appear again at Ge_{20} and Ge_{21}. The most stable configuration for Ge_{20} cluster is two stable Ge_9 isomers connected with a Ge_8 subunit, while the Ge_{21} cluster is a stack of three Ge_9 clusters. On the other hand, a compact configuration is found at the cluster Ge_{22}, which can be seen as an open-compact structure with two core atoms but with fewer bonds among atoms. For $n \geqslant 23$, the lowest-energy structures are constituted of compact stacks based on Ge_9. For example, the Ge_{24} can be seen as a unit of Ge_9 and Ge_{19}. Similar stacks of Ge_9 and open-compact structure are also found in Ge_{23} and Ge_{25}. Our present results suggest a competition between compact structures and stacked structures in the medium-sized clusters. Thus, as cluster size further increases, we expect that the germanium clusters will eventually adopt compact structure. During this transition, there should be a switch from prolate structure to near-spherical structure, which had been observed experimentally.[13]

IV. SIZE DEPENDENCE OF CLUSTER PROPERTIES

In Table I and Fig. 2, we compare the binding energy per atom, E_b, of the Ge_n clusters with experimental results. Reasonable agreement is obtained between theory and experiment. The discrepancy between theory and experiments is less than 0.02–0.2 eV for those clusters with $n=2$–25 and the size-dependent characters are also roughly reproduced by our calculations. As shown in Fig. 2, the cluster binding energies increase with cluster size n rapidly up to $n \leqslant 10$ and the size dependence become smooth at $n=14$–25. Such behavior can be related to the obtained structural transition around $n=11$–13. The equilibrium geometries undergo a transition from near-spherical structure to prolate geometry at $n=13$ (see Fig. 1). Experimentally, it was found that the Ge clusters with ~10–40 atoms follow a one-dimensional growth sequence and the prolate structures continue up to about 70.[13]

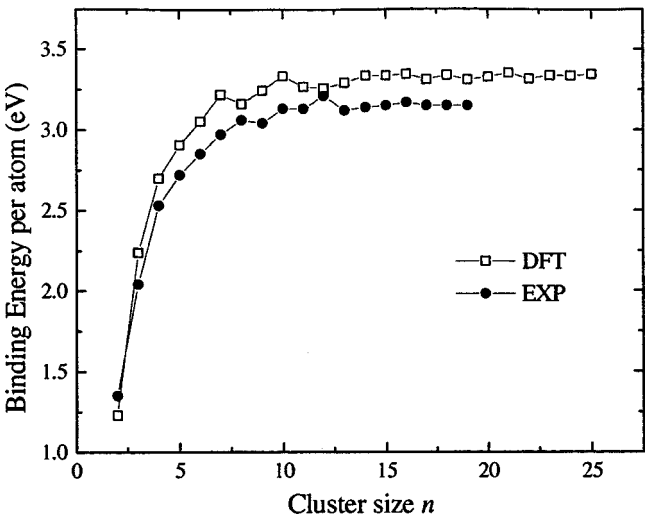

FIG. 2. Binding energies vs cluster sizes n for Ge_n. Circle: experimental results (Refs. 3 and 13). Square: DFT calculations.

In cluster physics, the second difference of cluster energies, $\Delta_2 E(n)=E(n+1)+E(n-1)-2E(n)$, is a sensitive quantity that reflects the stability of clusters and can be directly compared with the experimental relative abundance. Figure 3 shows the second difference of cluster total energies, $\Delta_2 E(n)$, as a function of the cluster size. Maxima are found at $n=4,7,10,14,16,18,21,23$, implying that these clusters are more stable than their neighboring clusters. The maxima at $n=10,14,16$ coincide with the experimental mass spectra[4–6] and the magic numbers at 4, 7, and 10 resemble those found for silicon clusters.[35,36] The relatively stable structures for the clusters with $n=14,16,18,21,23$ might be

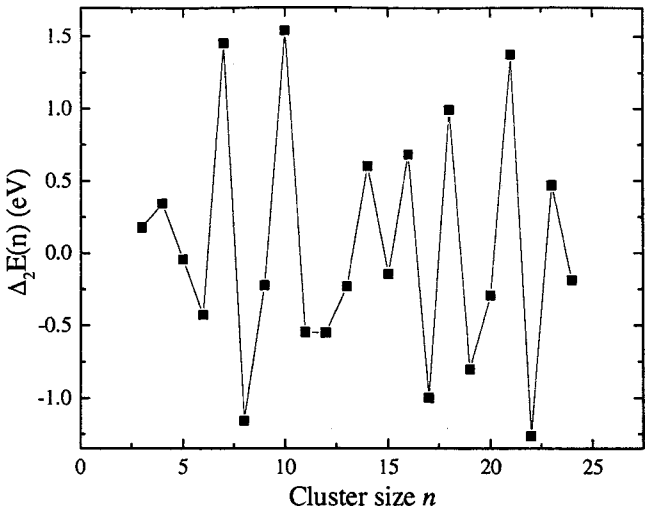

FIG. 3. Second differences of cluster energies $\Delta E(n)=E(n-1)+E(n+1)-2E(n)$ as a function of cluster size n for $n=2$–25.

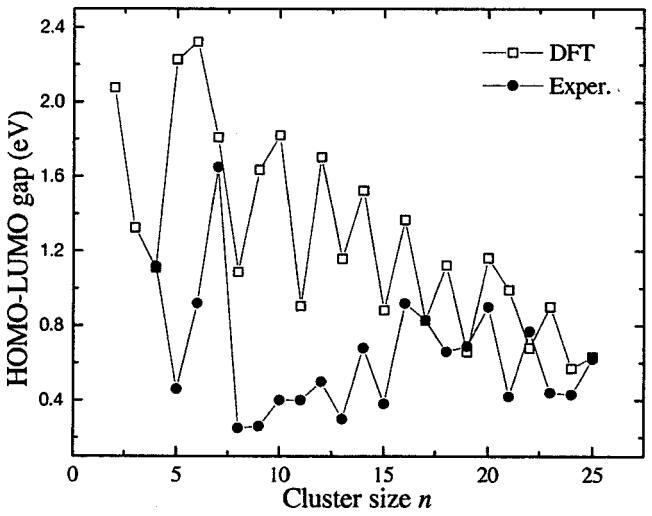

FIG. 4. HOMO-LUMO gap (eV) of Ge_n clusters. Circle: experiments (Refs. 11 and 37). Square: present DFT calculations.

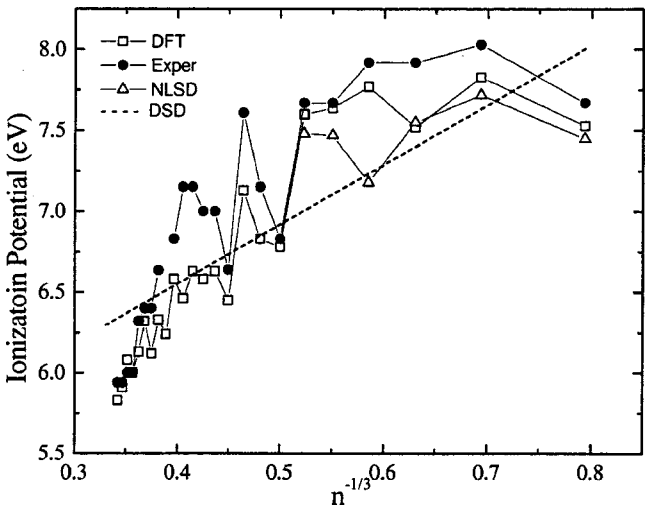

FIG. 5. Ionization potentials of Ge_n. Circle: experiments (Ref. 8). Square: our DFT calculations. Triangle: previous DFT results (Ref. 40). Dashed line: DSD model (Ref. 38).

explained in light of the details of the equilibrium structures of Ge_n. Since Ge_{10} is more stable than Ge_9, it is easy to understand that the Ge_{14} cluster constructed by a Ge_{10} and a Ge_4 square is more stable than the Ge_{13} cluster consisting of a Ge_9 and a Ge_3 triangle. The structures of Ge_{17} or Ge_{15} can be obtained adding or removing an atom from the Ge_{16} cluster. In the case of $n=18$, 21, 23, the layered structures with stable Ge_9 subunits are more stable than open-compact stacked structures with higher average coordination number.

We now discuss the electronic property of germanium clusters by examining the energy gap between the HOMO and LUMO. The low (high) electron affinity of a cluster is generally identified as a signature of a closed-shell (open-shell) pattern of electronic configuration with large (small) electronic gap. In previous experiments, Cheshnovsky *et al.* found that clusters with 4 and 7 atoms correspond to closed-shell electronic configurations and those with 3, 5, 9, and 12 atoms are open-shell species.[9] Burton *et al.* indicated that Ge_4, Ge_7, Ge_{11}, Ge_{14}, and, to a lesser extent, Ge_6 are closed-shell species with substantial HOMO-LUMO gaps.[10] Recently, Negishi *et al.* have estimated the HOMO-LUMO gap of Ge_n from the measured photoelectron spectra. Considerably large electronic gaps ($\geqslant 1.0$ eV) are found for Ge_4, Ge_6, and Ge_7,[11] and the gap decreases to 0.8–1.0 eV at about $n=30$.[37] The theoretical and experimental HOMO-LUMO gaps of Ge_n are compared in Fig. 4. Although our calculations somewhat overestimate the HOMO-LUMO gap,[37] the size-dependent trend is generally consistent with the experimental trend. The maxima at $n=10,12,14,16,20$ and minima at $n=8,13,15$ are reproduced by our calculations.

Another sensitive quantity to provide fundamental insight into the electronic structure is the ionization potential of the clusters.[38,39] In this work, we calculate the vertical ionization potentials from the total energy difference between the ground-state neutral Ge_n and the Ge_n^+ clusters. The theoretical results are given in Table I along with the experimental values.[8] In Fig. 5, the theoretical IP's of Ge_n are compared with the dielectric sphere droplet (DSD) model,[38] previous DFT results[40] as well as experimental data.[8] Our caclulation is consistent with experiments better than other theoretical results. The failure of the empirical DSD model implies that the small germanium clusters cannot be simply considered as a semiconductor sphere. The extremely high ionization potentials at $n=7,10$ further verify that the Ge_7 and Ge_{10} clusters are the most stable species.

V. CONCLUSIONS

The lowest-energy geometries, binding energies, HOMO-LUMO gap, and ionization potentials of Ge_n ($n=2-25$) clusters have been obtained by DFT-GGA calculations combined with a genetic algorithm. The germanium clusters follow a prolate growth pattern starting from $n=13$. The stacked layer structures are dominant in the size range of $n=13-18$. However, a near-spherical compact cagelike structure appears in the cluster Ge_{19}. The competition between compact structure and stacked layer structure leads to the alternative appearance of these two types of geometries. Stacked-compact structures are predominant for larger clusters. The second difference of cluster energies, HOMO-LUMO gap, and ionization potentials are calculated for the Ge_n clusters. Ge_n with $n=7,10$ are particularly stable than the open-packed structures (e.g., $n=8,11$) and the stacked layered structures consisting of the Ge_9 cluster are more stable than the compact structures. The calculated binding energies and ionization potentials are in agreement with the experimental values.

ACKNOWLEDGMENTS

The authors would like to thank for financial support the National Nature Science Foundation of China (No. 29890210), the U.S. ARO (No. DAAG55-98-1-0298), and NASA Ames Research Center. We acknowledge computational support from the North Carolina Supercomputer Center.

*Electronic address: ghwang@nju.edu.cn
†Electronic address: zhaoj@physics.unc.edu

[1] *Advances in Metal and Semiconductor Clusters*, edited by M.A. Duncan (JAI Press, Greenwich, 1993–1998), Vol. I–IV.
[2] *The Chemical Physics of Atomic and Molecular Clusters*, edited by G. Scoles (North-Holland, Amsterdam, 1990).
[3] J.E. Kingcade, H.M. Nagarathnanaik, I. Shim, and K.A. Gingerich, J. Phys. Chem. **90**, 2830 (1986); K.A. Gingerich, M.S. Baba, R.W. Schmude, and J.E. Kingcade, Chem. Phys. **262**, 65 (2000); K.A. Gingerich, R.W. Schmude, M.S. Baba, and G. Meloni, J. Chem. Phys. **112**, 7443 (2000).
[4] T.P. Martin and H. Schaber, J. Chem. Phys. **83**, 855 (1985).
[5] J.C. Phillips, J. Chem. Phys. **85**, 5246 (1986).
[6] W. Schulze, B. Winter, and I. Goldenfeld, J. Chem. Phys. **87**, 2402 (1987).
[7] J.R. Heath, Y. Liu, S.C. O'Brien, Q.L. Zhang, R.F. Curl, F.K. Tittel, and R.E. Smalley, J. Chem. Phys. **83**, 5520 (1985); Q.L. Zhang, Y. Liu, R.F. Curl, K.F. Kittel, and R.E. Smalley, *ibid.* **88**, 1670 (1988).
[8] S. Yoshida and K. Fuke, J. Chem. Phys. **111**, 3880 (1999).
[9] O. Cheshnovsky, S.H. Yang, C.L. Pettiette, M.J. Craycraft, Y. Liu, and R.E. Smalley, Chem. Phys. Lett. **138**, 119 (1987).
[10] G.R. Burton, C.S. Xu, C.C. Arnold, and D.M. Meumark, J. Chem. Phys. **104**, 2757 (1996).
[11] Y. Negishi, H. Kawamata, T. Hayase, M. Gomei, R. Kishi, F. Hayakawa, A. Nakajima, and K. Kaya, Chem. Phys. Lett. **269**, 199 (1997).
[12] M.F. Jarrold and V.A. Constant, Phys. Rev. Lett. **67**, 2994 (1991).
[13] J.M. Hunter, J.L. Fye, M.F. Jarrold, and J.E. Bower, Phys. Rev. Lett. **73**, 2063 (1993).
[14] I. Rata, A.A. Shvartsburg, M. Horoi, T. Frauenheim, K.W.M. Siu, and K.A. Jackson, Phys. Rev. Lett. **85**, 546 (2000).
[15] *Tight-binding molecular dynamics*, edited by L. Colombo [Comput. Mater. Sci. **12**, Issue 3 (1998)].
[16] L. Mitas, J.C. Grossman, I. Stich, and J. Tobik, Phys. Rev. Lett. **84**, 1479 (2000).
[17] A.A. Shvartsburg, B. Liu, Z.Y. Lu, C.Z. Wang, M.F. Jarrold, and K.M. Ho, Phys. Rev. Lett. **83**, 2167 (1999).
[18] J.L. Wang, J.J. Zhao, F. Ding, W.F. Shen, H. Lee, and G.H. Wang, Solid State Commun. **117**, 593 (2001).
[19] J.J. Zhao, J.L. Wang, and G.H. Wang, Phys. Lett. A **275**, 281 (2000).
[20] M. Menon, J. Phys.: Condens. Matter **10**, 10 991 (1998).
[21] K. Balasubramanian, J. Mol. Spectrosc. **139**, 405 (1990); D. Dai, K. Sumathi, and K. Balasubramanian, Chem. Phys. Lett. **193**, 251 (1992); D. Dai and K. Balasubramanian, J. Chem. Phys. **96**, 8345 (1992); **105**, 5901 (1996).
[22] G. Lanza, S. Millefiori, A. Millefiori, and M. Dupuis, J. Chem. Soc., Faraday Trans. **89**, 2961 (1993).
[23] P.W. Deutsch, L.A. Curtiss, and J.P. Blaudeau, Chem. Phys. Lett. **270**, 413 (1997).
[24] E.F. Archibong and A. St-Amant, J. Chem. Phys. **109**, 962 (1998).
[25] S. Ogut and J.R. Chelikowsky, Phys. Rev. B **55**, 4914 (1997).
[26] B.X. Li and P.L. Cao, Phys. Rev. B **62**, 15 788 (2000).
[27] Z.Y. Lu, C.Z. Wang, and K.M. Ho, Phys. Rev. B **61**, 2329 (2000).
[28] DMOL is a density-functional theory package distributed by MSI. B. Delley, J. Chem. Phys. **92**, 508 (1990).
[29] J.P. Perdew and Y. Wang, Phys. Rev. B **45**, 13 244 (1992).
[30] Y. Wang and J.P. Perdew, Phys. Rev. B **43**, 8911 (1991).
[31] D.M. Deaven and K.M. Ho, Phys. Rev. Lett. **75**, 288 (1995); D.M. Deaven, N. Tit, J.R. Morris, and K.M. Ho, Chem. Phys. Lett. **256**, 195 (1996).
[32] Y.H. Luo, J.J. Zhao, S.T. Qiu, and G.H. Wang, Phys. Rev. B **59**, 14 903 (1999); T.X. Li, S.Y. Yin, Y.L. Ji, B.L. Wang, G.H. Wang, and J.J. Zhao, Phys. Lett. A **267**, 403 (2000); J.J. Zhao, Y.H. Luo, and G.H. Wang, Eur. Phys. J. D **14**, 309 (2001).
[33] B.L. Wang, S.Y. Yin, G.H. Wang, A. Buldum, and J.J. Zhao, Phys. Rev. Lett. **86**, 2046 (2001).
[34] K.M. Ho, A.A. Shvartsburg, B.C. Pan, Z.Y. Lu, C.Z. Wang, J.G. Wacker, J.L. Fye, and M.F. Jarrold, Nature (London) **392**, 582 (1998).
[35] K. Raghavachari and C.M. Rohlfing, J. Chem. Phys. **89**, 2219 (1988).
[36] A. Bahel and M.V. Ramakrishna, Phys. Rev. B **51**, 13 849 (1995); J. Pan, A. Bahel, and M.V. Ramakrishna, Mod. Phys. Lett. A **9**, 811 (1995).
[37] Y. Negishi, H. Kawamata, F. Hayakawa, A. Nakajima, and K. Kaya, Chem. Phys. Lett. **294**, 370 (1998).
[38] G. Makov, A. Nitzan, and L.E. Brus, J. Chem. Phys. **88**, 5076 (1988).
[39] J.J. Zhao, M. Han, and G.H. Wang, Phys. Rev. B **48**, 15 297 (1993).
[40] P. Jackeson, K.J. Fisher, G.E. Gadd, I.G. Dance, D.R. Smith, and G.D. Willett, Int. J. Mass Spectrom. Ion Processes **164**, 45 (1997).